

Time Dependent Process-Zone Growth in Polycarbonate

Amkee Kim* and Sam-Hong Song**

(Received December 1, 1994)

The process zone evolution strongly influences the crack growth of polycarbonate. A methodology for determination of the kinetics of the process zone evolution was developed by decoupling these two process. Constant displacement (stress relaxation) conditions under which the crack length remained. A thermodynamic model for equilibrium process zone in polycarbonate is developed from the modification of Chudnovsky model. Based on the model the driving force and a new kinetic equation for evolution of the process zone are proposed after considering of the irreversible thermodynamics and chemical reaction theories. In addition, the validity of model and new kinetic equation are examined experimentally.

Key Words : Crack, Process Zone, Polycarbonate, Kinetics, Thermodynamic Equilibrium

1. Introduction

Numerous authors have reported that slow-crack propagation in polycarbonate (PC) is commensurate with the formation and growth of a process zone surrounding the crack (Donald et al., 1981; Nisitani et al., 1985; Haddaoui et al., 1986; Stojimirovic and Kadota et al., 1992). The energy required for process zone growth can be many orders of magnitude greater than the surface energy associated with crack formation and as such can provide significant resistance to crack growth. Thus the kinetics of the process zone development is an essential factor in the time dependent fracture behavior analysis of PC.

A thermodynamic model for an equilibrium process zone in polymers was proposed by Chudnovsky (Stojimirovic and Chudnovsky, 1992) and its validity has been supported by the experimental studies on various polyethylenes (Kadota et al., 1991; Stojimirovic et al., 1992). The essence of the Chudnovsky

Model (CM) is that the process zone can be considered as a homogeneous second phase, i.e., transformed material, and thus the shape and the size of the process zone are derived from the phase equilibrium conditions. However, the observation of the process zone in polycarbonate (PC) shows an important difference: It consists of shear bands whose density varies noticeably within the zone.

In the present paper, we modify the CM to account for the variable extent of transformation of material within the process zone, based on the experimental observation, and construct a constitutive equation for process zone growth employing thermodynamic consideration. We employ the modified Chudnovsky Model (CM) to determine the process zone driving force and then formulate an appropriate kinetic equation following the frame work of irreversible thermodynamics.

Finally the validity of newly formulated constitutive equation for PC process zone evolution is examined by experimental data.

2. Experiment

2.1 Material and specimen preparation

Polycarbonate of molecular weight, M_w 38000, Caliber 300-3, was provided by the Dow Chemi-

* Department of Mechanical Engineering, Kongju National University, 182 Shinkwan-dong, Kongju, Chungnam, Korea

** Department of Mechanical Engineering, Korea University, 5-1 Anam-dong, Sungbok-ku, Seoul, Korea

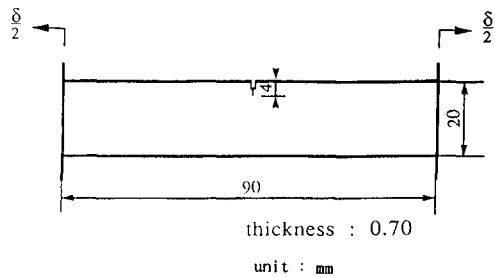


Fig. 1 Dimensions of SEN specimen. $\delta/2$ represents the applied displacement at grip points.

cal Company in the form of injection molded plaques of 3 mm thickness. After drying in a vacuum oven at 120°C for 24 hours, the plaques were further compressed to 0.7 mm thickness using a Dake compression molder under the following conditions; preheat to 270°C, hold at zero load for 10 minutes, compression under 4 MN/m² for 5 minutes, then another 8 minutes under this same compression condition until cooled to 23°C. Single edge notched (SEN) specimens of dimensions shown in Fig. 1 were machined from the compression molded plaques.

2.2 Kinetics of process zone growth under fixed displacement

The SEN specimens were strained in tension to fixed displacements, $\delta = 1.00, 1.15, 1.25$ and 1.35 mm, at a constant cross-head speed of 0.6 mm/sec at 23°C, then held at constant strain. The load was monitored throughout the test. The kinetics of the process zone evolution was monitored through a video-recording system attached to a microscope. The process zone size is reconstructed from a combination of a side view from the video screen (Fig. 2(a)) and optical microscopy of cross-section parallel to the direction of load application.

3. Observation

Figure 2(a) and b are examples of an actual determination of the process zone shape and size from the side view and cross-sections A-A' (normal to the crack plane). These two projections allow the determination of the process zone

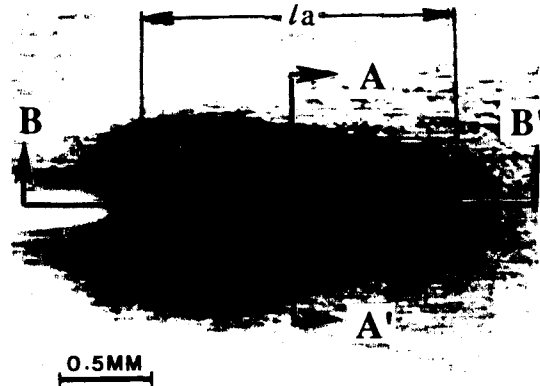
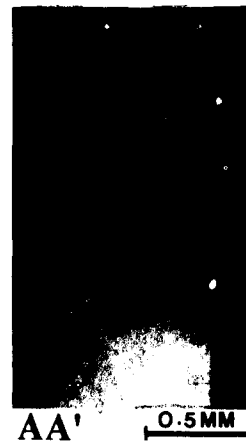


Fig. 2 (a) A side-view of process zone from the video screen. l_a represents the length of process zone.



(b) Cross-section A-A' in polarized transmitted light.

dimensions. It is obvious from Fig. 2(b) (cross-section A-A') that there is thinning in the thickness direction. In addition, two families of intersecting shear bands are observed. The final equilibrium process zone size is determined based on the side-view, the thinning profile and fracture surface (cross-section B-B').

The stress-relaxation behavior during the test is given in Fig. 3. The dashed lines indicate the values of remote stress, σ_∞ , at an apparent equilibrium. This stress behavior is utilized in the computation of model and driving force.

The kinetics of the process zone evolution is depicted in Fig. 4 which shows the process zone length, l_a , versus time for SEN specimens for the

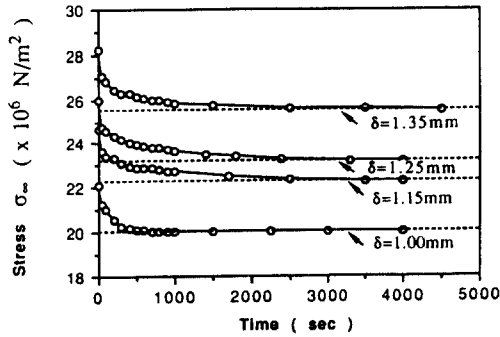


Fig. 3 Stress relaxation data at various displacements in SEN.

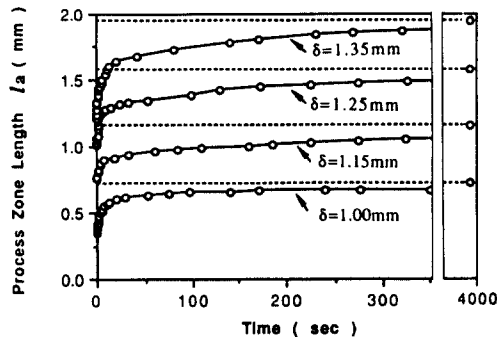


Fig. 4 Process zone length, l_a (mm), vs time(sec).

four experimental conditions described previously. The process zone is seen to reach at least half of its final length during the initial ramp loading and then follows an increasingly slower approach to an apparent equilibrium size $l_{a(eq)}$ dependent on the displacement. The dashed lines in Fig. 4 represent the values of the equilibrium sizes. Some relatively small crack growth from the notch-tip occurred during the initial loading and for a short period thereafter, particularly at the highest strain loading. However, the crack is arrested soon after the stress relaxation starts and remains stationary during subsequent process zone evolution. Thus this process occurs at essentially constant crack length. Fig. 4 represents the process zone evolution data acquired at this stage.

4. Review of Chudnovsky Model (CM)

A thermodynamic model for an equilibrium process zone in polymers was proposed by Chud-

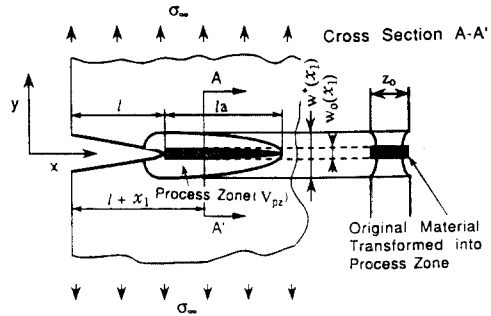


Fig. 5 Schematic diagram of a crack and process zone in polycarbonate

novsky (Stojimirovic and Chudnovsky, 1992). The essence of the Chudnovsky Model (CM) is that the process zone can be considered as a homogeneous second phase, i. e., transformed material, and thus the shape and the size of the process zone are derived from the phase equilibrium conditions.

Let G be the Gibbs potential of the system described in Fig. 5 and V_{pz} be the domain occupied by the process zone. Then for isothermal condition the equilibrium domain V_{pz} of the process zone corresponds to the minimum of G , i. e. :

$$\frac{\delta G(\sigma_{\infty}, V_{pz})}{\delta V_{pz}} \Big|_{t=const} = 0 \quad (1)$$

Here, G is a functional of the domain V_{pz} and a function of crack length l and applied stress σ_{∞} . Following the reference (Stojimirovic and Chudnovsky, 1992), we employ the Eshelby method to evaluate a variation of the Gibbs potential due to a virtual migration of the process zone boundary :

$$\delta G = - \int_{\delta V_{pz}} \delta \xi_i (P_{ij}^o - P_{ij}^{pz}) n_j d\Gamma \quad (2)$$

For evaluation of the Gibbs potential, G , of a crack with the surrounding process zone consisting of the second phase (see Fig. 6(a)), the two-phase system was decomposed into its elements as shown in Fig. 6(b). The first element results from removal of the process zone and substituting its action with an equivalent traction σ_{dr} along the interface (σ_{dr} is the drawing stress). The second element is the process zone V_{pz} within which the original material submitted to σ_{dr} undergoes the transformation (drawing). The width, $w_0(x_1)$, of

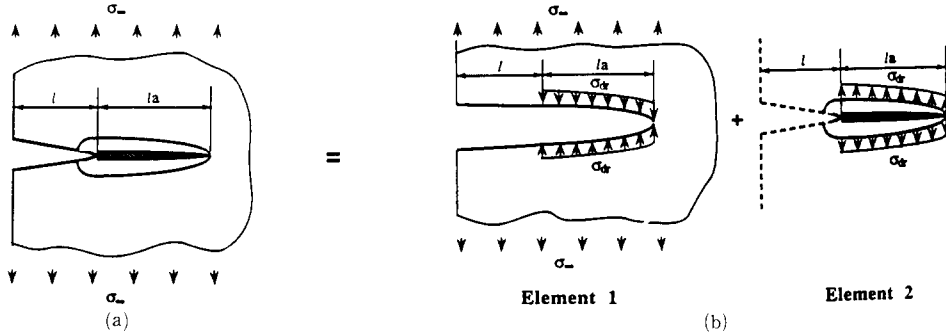


Fig. 6 A model for the computation of Gibbs potential : Element one is obtained from removal of the process zone and substituting its action with an equivalent traction σ_{dr} along the interface, and element two is obtained from the process zone V_{pz} within which the original material submitted to σ_{dr} undergoes the transformation

the layer of the original material in Fig. 5 that underwent transformation varies along the process zone length and is initially unknown. The resulting width, $w^*(x_1)$, of the process zone is $w^*(x_1) = \lambda(x_1)w_0(x_1)$, with λ being the draw ratio and assumed constant within the process zone. The displacement caused by the transformation at the interface shown in element 2 of Fig. 6(b) is $w^*(x_1) - w_0(x_1)$.

For coherency of the interface, it is required that the opening of a slit in element 1 be equal to the displacement of the boundary of element 2. For a slender process zone, the displacement of element 1 can be approximated as the crack-opening displacement, Δ , thus leading to the following compatibility equation :

$$\Delta(x_1, l, l_a) = w^* - w_0 \tag{3}$$

Then, the width $w_0(x_1)$ of the initial strip that is transformed into the process zone is directly related to the crack-opening displacement of element 1 in Fig. 6(b) :

$$w_0(x_1) = \Delta(x_1, l, l_a)(\lambda - 1)^{-1} \tag{4}$$

Thus, the volume V_{pz} of the initial material can be expressed as

$$V_{pz} = z_0 \int_l^{l+l_a} \Delta(x_1, l, l_a)(\lambda - 1)^{-1} dx_1 \tag{5}$$

where z_0 is the initial thickness of the specimen. The process-zone shape is thus uniquely determined by the process zone length, l_a , because the crack-opening displacement depends on constants

l , σ_{∞} , σ_{dr} , and a variable l_a . Thus the condition for the minimum Gibbs potential for two-phase system equilibrium (Eq. 1) can be written as :

$$\left. \frac{dG(\sigma_{\infty}, l, l_a, \sigma_{dr}, \lambda)}{dl_a} \right|_{t=const} = 0 \tag{6a}$$

$$\left. \frac{d^2G}{dl_a^2} \right|_{t=const} > 0 \tag{6b}$$

Here λ is draw ratio. The equation 6a leads to the following equation (Stojimirovic and Chudnovsky, 1992) :

$$K^{tot}(K^{tot} + \gamma K(\sigma_{dr})) = 0 \tag{6c}$$

and the inequality equation 6b ensures the uniqueness of the solution, i. e. :

$$K^{tot} + \gamma K(\sigma_{dr}) = 0 \tag{7}$$

Here K^{tot} is the stress intensity factor (SIF) for the element 1 of Fig. 6(b). $K(\sigma_{dr})$ is the SIF for the same element with absence of σ_{∞} . γ represents $2\gamma^*/((\lambda - 1)\sigma_{dr})$ where γ^* is the specific transformation energy. This solution leads to the equilibrium process zone size and shape which agree well with experimental observations on polyethylene and thin film polycarbonate (Kadota, 1991 et al.; Stojimirovic and Kadota et al., 1992; Stojimirovic and Chudnovsky, 1992).

5. Modification of Chudnovsky Model (CM) for Polycarbonate

As mentioned previously, polycarbonate was observed to undergo non-homogeneous transfor-

mation within the process zone. Fig. 2(b) shows the optical micrograph in polarized light and the two intersecting families of shear bands in cross section A-A'. We consider the individual shear band as transformed material. Between the shear bands the material appears to be untransformed. During the evolution of the process zone, drawing progresses by (a) an increase of the number of shear bands, and (b) increase of the width of the individual shear bands at the expense of the neighboring untransformed material (Ma et al., 1989). The various stages of drawn state correspond to different densities of shear bands.

To characterize an intermediate transformation we introduce an extent of transformation ζ . $\zeta=0$ corresponds to the original state and $\zeta=1$ is associated with the fully transformed state. The thinning of cross-section is a cumulative effect of the shear banding as illustrated in Fig. 2(b). The thinning and the draw ratio, λ , are uniquely related since the density of transformed material is practically unchanged (a few percent)(Kadota et al., 1991). The extent of transformation, ζ , is simply related to the draw ratio λ which can be estimated by measuring the thinning (Kim, A. et al., 1993 b):

$$\zeta = \left(\frac{\lambda - 1}{\lambda} \right) \left(\frac{\lambda^*}{\lambda^* - 1} \right) \quad (8)$$

where λ^* is the draw ratio for fully transformed material which is a constant and λ is a variable draw ratio reflecting a current extent of transformation. The distributions of $\zeta(x_1/l_a)$ differ for a process zone formed under different conditions. $\zeta(x_1/l_a)$ can be approximated experimentally (Kim, A. et al., 1993 a).

Thus the Eq. 6a which is the necessary condition of the minimum Gibbs potential is rewritten as :

$$\frac{\partial G}{\partial l_a} \Big|_{l=const} + \frac{\partial G}{\partial \zeta} \frac{d\zeta}{dl_a} \left(\frac{x_1}{l_a} \right) = 0 \quad (9)$$

The Eq. 9 determines the size of equilibrated process zone. Figure 7 shows the solution of the Eq. 9(solid line) with $\gamma^* = 7.05 \times 10^6 \text{ J/m}^3$ for the various fixed displacement conditions. The experimental data points are shown by the open circles.

Only one parameter is employed in the above treatment for the four experimental condition reported. The justification of this value comes from independent tests using the neck formation in simple tension combined with calorimetric determination of the residual strain energy stored in the transformed (necked) material and estimation of heat generation during the transformation.

6. Driving Force for Evolution of the Process Zone

The driving force on an interface between original material and the process zone can be defined following Eshelby, 1970. In our case, the evolution of the interface is uniquely determined

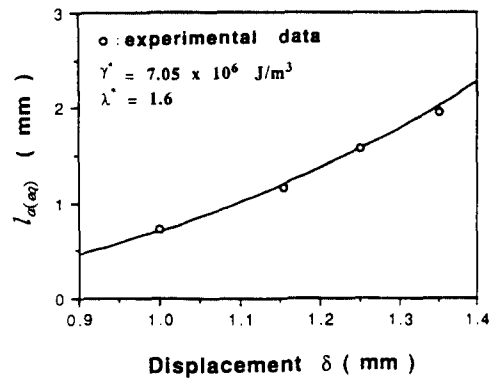


Fig. 7 Equilibrated process zone length, $l_a(eq)$, as a function of applied displacements. The solid line represents the theoretical solution

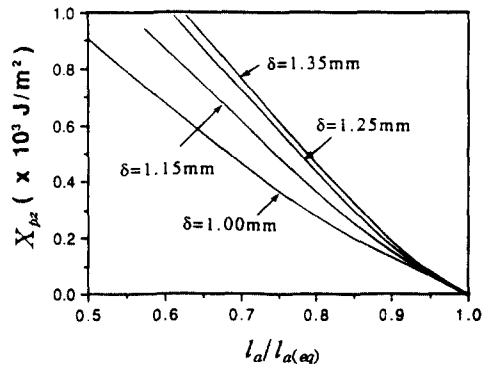


Fig. 8 Process zone driving force, X_{pz} , as function of process zone length normalized by the apparent equilibrated process zone length, $l_a/l_a(eq)$, for various applied displacements

by the process zone length, l_a , as a function of time. The driving force X_{pz} is determined as:

$$X_{pz} = - \left. \frac{dG}{dl_a} \right|_{t=const} \quad (10)$$

Since the Gibbs potential G is dependent on ζ (x_1/l_a) as well as l_a , the process zone driving force can be presented as:

$$X_{pz} = - \left[\left. \frac{\partial G}{\partial l_a} \right|_{t=const} + \frac{\partial G}{\partial \zeta} \frac{d\zeta}{dl_a} \left(\frac{x_1}{l_a} \right) \right] \quad (11)$$

Figure 8 shows the dependency of the process zone driving force as a function of $l_a/l_{a(eq)}$ for the four experimental displacement conditions. At equilibrium the process zone driving force is zero.

7. The Kinetic Equation of Process Zone Evolution

In irreversible thermodynamics for system close to equilibrium the rate of change toward the equilibrium is assumed to be proportional to the corresponding driving force, X . In our case the rate of approaching equilibrium is defined by the rate of changes in l_a , i. e., \dot{l}_a . Thus a kinetic equation can be written as:

$$\dot{l}_a = kX_{pz} \quad (12)$$

The Arrhenius equation was first developed to account for the temperature dependency of the reaction rate constant, k , in chemical kinetics. Since the Eq. 12 resembles that of a first order chemical reaction and so adapting the Arrhenius assumption of k with incorporation of an activation energy, U , reduced by the process zone driving force, X_{pz} , we propose the following equation for the kinetic coefficient in the Eq. 12:

$$k = k_o \exp \left(- \frac{U - \alpha X_{pz}}{RT} \right) \quad (13)$$

where T is the absolute temperature, R is the gas constant, k_o is a material constant with unit of $m^4/(J\text{-sec})$, and α is also a material constant with unit m^2/mole . Finally, combining the Eqs. 12 with 13 we arrive at a new kinetic equation as follows:

$$\dot{l}_a = \left[k_o \exp \left(- \frac{U - \alpha X_{pz}}{RT} \right) \right] X_{pz} \quad (14)$$

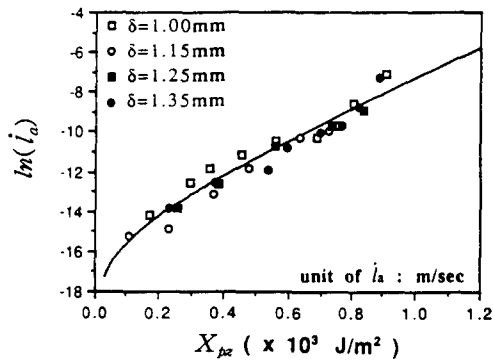


Fig. 9 A master curve for polycarbonate process zone kinetics. \dot{l}_a represents the process zone growth rate.

Note that the Eq. 14 accounts for an equilibrated state ($\dot{l}_a=0$ when $X_{pz}=0$) and becomes increasingly nonlinear with increasing X_{pz} , that is to say with increasing departure from the equilibrium.

Since the experiments reported in this paper were performed at one temperature the equation is simplified and the data cast as $\ln(\dot{l}_a)$ versus X_{pz} in Fig. 9. The solid line indicates the fit of Eq. 14 with a constant α as $16.39 \times 10^3 (m^2/kmol)$. The strongly nonlinear kinetics data are now collapsed into a master curve.

8. Conclusion

(1) An experimental procedure for the study of the kinetics of the process zone evolution decoupled from the kinetics of crack growth for polycarbonate was designed and implemented. This was achieved by observing the process zone evolution under stress-relaxation at essentially constant crack length.

(2) An modification of the Chudnovsky Model (CM) is made which accounts for non-homogeneous transformation of material within a process zone surrounding a crack. The distribution of the extent of transformation was experimentally determined in these studies. Further generalization of the model using the variation of Gibbs potential should allow for prediction of the distribution without experimental determination.

(3) The driving force for the process zone evolution is evaluated and a new kinetic equation

incorporating the driving force is proposed which leads to a master curve for the observed growth of the process zone under various loading histories.

References

- Atkins, A. G., Lee, C. S. and Cadell, R. M., 1975, "Time-Temperature Dependent Fracture Toughness of PMMA," *Journal of Material Sci.*, Vol. 10, pp. 1381~1393.
- Donald, A. M. and Kramer, E. J., 1981, "Micromechanics and Kinetics of Deformation Zones at Crack Tips in Polycarbonate," *Journal of Material Sci.*, Vol. 16, pp. 2977~2987.
- Eshelby, J. D., 1970, "*Inelastic Behavior of Solid*," McGraw-Hill, pp. 77~115.
- Haddaoui, N., Chudnovsky, A. and Moet, A., 1986, "Ductile Fatigue Crack Propagation in Polycarbonate," *Polymer*, Vol. 27, pp. 1377~1384.
- Kadota, K. and Chudnovsky, A., 1991, "A New Thermodynamic Model for a Process Zone in Polymers," *Proc. of ASME Winter Annual Meeting, MD29*, pp. 101~114.
- Kim, A., Garrett, L. V., Bosnyak, C. P. and Chudnovsky, A., 1993, "Modeling the Process-Zone Kinetics of Polycarbonate," *Journal of Applied Polymer Sci.*, Vol. 49, pp. 885~892.
- Kim, A., Garrett, L. V., Bosnyak, C. P. and Chudnovsky, A., 1993, "Kinetics and Characterization of the Process Zone Evolution in Polycarbonate," *Journal of Applied Polymer Sci.*, Vol. 49, pp. 885~892.
- Lee, O. S., 1985, "Tertiary Ductile Fracture Process in Polycarbonate(PC) specimens," *Journal of Materials Sci. Letters*, Vol. 4, pp. 125~128.
- Ma, M., Vijayan, K., Hiltner, A., Baer, E. and Im, J., 1989, "Shear Yielding Modes of Polycarbonate," *Journal of Material Sci.*, Vol. 24, pp. 2687~2696.
- Nisitani, H. and Hyakutake, H., 1985, "Condition for Determining the Static Yield and Fracture of Polycarbonate Plate Specimen with Notch," *Eng. Fracture Mechanics*, Vol. 22, pp. 359~368.
- Stojimirovic, A. and Chudnovsky, A., 1992, "A New Thermodynamic Model for a Process Zone in Polymers," *Int. J. of Fracture*, Vol. 57, pp. 281~289.
- Stojimirovic, A., Kadota, K. and Chudnovsky, A., 1992, "An Equilibrial Process Zone in Polymeric Materials," *Journal of Applied Polymer Sci.*, Vol. 46, pp. 1051~1056.